The genotype 3-specific hepatitis C virus core protein residue phenylalanine 164 increases steatosis in an in vitro cellular model.

Christophe Hourioux, Romuald Patient, Aurélie Morin, Emmanuelle Blanchard, Moreau Alain, Sylvie Trassard, Bruno Giraudeau, Philippe Roingeard

GUT 2007, **56,** 1302-1308.

The genotype 3-specific hepatitis C virus core protein residue phenylalanine 164 increases steatosis in an *in vitro* cellular model

C Hourioux, R Patient, A Morin, E Blanchard, A Moreau, S Trassard, B Giraudeau, P Roingeard

Correspondence to: Prof. Philippe Roingeard, INSERM ERI 19, Laboratoire de Biologie Cellulaire, Faculté de Médecine, Université François Rabelais de Tours, 10 boulevard Tonnellé, F-37032 Tours Cedex France.

Tel (33) 2 47 36 60 71 - Fax (33) 2 47 36 60 90 - E-mail: roingeard@med.univ-tours.fr

Authors' affiliations:

C Hourioux, R Patient, A Morin, E Blanchard, A Moreau, S Trassard, P Roingeard, Université François Rabelais, INSERM ERI 19 & CHRU de Tours, France.

B Giraudeau, Université François Rabelais, INSERM CIC 0202 & CHRU de Tours, France.

Running title: HCV genotype 3-specific steatosis

Keywords: HCV, genotype, steatosis, lipid droplet

Abbreviations: HCV, hepatitis C virus; ER, endoplasmic reticulum; SPP, signal peptide peptidase; SFV, Semliki forest virus; EM, electron microscopy; MTP, microsomal triglyceride transfer; apoB, apolipoprotein B; VLDL, very low density lipoproteins; PDI, protein disulphide isomerase; β-Gal, β-galactosidase

Abstract

Background and aims: The prevalence and severity of liver steatosis are higher in patients infected with genotype 3 hepatitis C virus (HCV) than in patients infected with other genotypes. HCV core protein is known to affect lipid metabolism, inducing lipid droplet accumulation both *in vitro* and *in vivo*. We used an *in vitro* cellular model to investigate whether an HCV core protein with residues specific to genotype 3 increased this phenomenon.

Methods: Sequence comparisons for HCV core protein domain II, which is known to interact with lipid droplets, identified the phenylalanine (F) residue at position 164 as the only residue specific to genotype 3. We compared the area covered by lipid droplets in sections of cells producing a wild-type genotype 1a HCV core protein with that in cells producing a Y164F mutant protein.

Results: Cumulative lipid droplet area was significantly greater in sections of cells producing the Y164F mutant HCV core protein than in cells producing the wild-type protein ($p<0.001$). The frequency of cell sections containing more than 3 μm^2 of lipid droplets, in particular, was higher for the mutant than for the wild-type protein.

Conclusion: Our data provide a molecular explanation for HCV genotype 3-specific lipid accumulation. This difference between genotypes may be due to phenylalanine having a higher affinity for lipids than tyrosine (Y). These observations provide useful information for further studies of the mechanisms involved in HCV-induced steatosis.

Hepatitis C virus (HCV), a member of the *Flaviridae* family, is a major cause of chronic liver disease, infecting an estimated 170 million people worldwide.[1] Comparisons of the nucleotide

sequences of variants recovered from infected individuals in different risk groups for infection and from different geographical regions has revealed the existence of six major genetic groups, called genotypes.[2] Each of these six genotypes consists of a series of more closely related subtypes, differing in nucleotide sequence by 20 to 25%, whereas differences of more than 30% are observed between genotypes.[2] Most HCV-associated liver injury results from the host immune response,[3] but some pathological features, such as liver steatosis, are compatible with direct viral cytopathic effects contributing to disease progression.[4 5] Steatosis involves the deposition of triglycerides in the liver and constitutes a major determinant of the progression of fibrosis in patients with chronic hepatitis.[6 7] Liver steatosis may be related to host metabolic factors (excess weight, diabetes, hyperlipidaemia, excessive alcohol intake),[8-10] but many studies have clearly demonstrated a significant association between HCV genotype 3 infection and the presence of steatosis.[11-14] The prevalence and severity of steatosis are higher in patients infected with HCV of genotype 3 than in patients infected with other HCV genotypes. In patients infected with genotype 3 viruses, fat accumulation in the liver is correlated with the level of HCV replication in the serum[13] and liver[9], and disappears following successful antiviral therapy.[14 15] Conversely, most cases of mild steatosis in patients infected with other genotypes seem to be metabolic in origin, with excess weight being the most significant clinical correlate.[16] Steatosis usually persists following successful antiviral therapy in patients infected with a non-genotype 3 HCV.[15 17] These clinical observations suggest that specific genotype 3 HCV products may be involved in liver steatosis.

In vitro studies have shown that HCV core protein can associate with lipid droplets acting as intracellular storage sites for triacylglycerols and cholesterol esters.[18-21] Two lines of transgenic mice producing HCV core protein exclusively in the liver develop steatosis, followed by hepatocellular carcinoma.[22 23] Until recently,[24] studies on HCV core protein production were based on the use of constructs derived from isolates of HCV genotype 1. We have established a model based on Semliki forest virus (SFV) replicon vectors, which can be used to produce HCV core protein in mammalian cells, leading to the assembly of this protein into HCV-like particles.[25-27] Although this cellular model is based on HCV core protein production from a genotype 1a virus, it also displays the accumulation and clustering of lipid droplets in the perinuclear area of transfected cells, mimicking HCV core protein-associated steatosis *in vitro*.[27] We therefore studied the role of HCV genotype in steatosis, by investigating whether the production of a core protein bearing residues specific to HCV genotype 3 increased lipid droplet clustering and accumulation in this *in vitro* cellular model.

METHODS

Sequence alignment and construct design

The HCV core protein has three domains, based on predicted structural and functional characteristics (fig. 1).[20 28] Domain I, corresponding to the first 120 amino acids (aa) at the N-terminus, is a highly basic domain, probably involved in recruiting viral RNA for particle morphogenesis. Domain II, located between amino acids 120 and 179 (approximate position), is a hydrophobic region predicted to form one or two α-helices involved in the association of the core with the ER membrane and lipid droplets. Domain III, corresponding to the C-terminal 20 aa of the protein, is a highly hydrophobic region that serves as a signal sequence for targeting the viral glycoprotein E1 to the endoplasmic reticulum (ER). Cleavage by a signal peptidase in the ER lumen releases the N-terminal end of E1 from the viral polyprotein, leaving the 191 aa core protein anchored by the signal peptide.[29] This 191 aa polypeptide (p23) is further processed by an intramembrane protease, the signal peptide peptidase (SPP), which cleaves within the C-terminal signal peptide, releasing the N-terminal 173-179 aa of the core protein from the ER.[29] This cleaved core protein (p21) is then available for association with lipid droplets.[29] We focused our sequence variability analysis on domain II, because this sequence is involved in the association of HCV core protein with lipid droplets (fig. 1A). Core protein sequences of the six HCV genotypes, including 25 subtypes, were extracted and analysed through the web-accessible search interface of the Los Alamos National Laboratory (USA) HCV database (http://hcv.lanl.gov).[30] We found that the phenylalanine (F) in position 164 of HCV core protein was the only residue specific to genotype 3 sequences (fig. 1A). This residue was present in 24 of 33 genotype 3 sequences (73%), whereas a tyrosine (Y) residue was present in position 164 in sequences from all other genotypes (fig. 1A). We therefore decided to replace Y164 by F in a core protein sequence from an HCV 1a genotype.

The HCV core 1a construct was obtained from our previously described[25] genotype 1a cDNA clone (Dj6.4; Genbank accession number AF529293), containing the C-E1-E2 coding sequence. The domain II sequence of the core protein encoded by this clone is identical to the consensus core protein sequence for genotype 1a shown in fig. 1a. The sequence encoding the HCV core protein (C191 aa) and the first 27 aa at the N-terminus of the E1 protein were amplified from the Dj6.4 cDNA by PCR, using a specific set of oligonucleotide primers, consisting of the forward primer (5' GTGGATCCTGCACC***ATG***AGCACGAATCCT 3') and the reverse primer (5 'ACATGCTCTGCCGGCTA***ATTACT***CCTAGGAGAC 3'). The start codon and inserted stop codons are indicated in bold, italic typeface. *Bam*H1 sites were also

included in the primer sequences (underlined), for subcloning in pSFV1 (Invitrogen). A codon yielding the genotype 3 core protein-specific residue at position 164 was introduced into this sequence by mutation. The tyrosine in position 164 was thus converted into a phenylalanine (Y164F). This site-directed mutagenesis was performed with internal primers 5' CGGCGTGAACT**T**TGCAACAGGG 3' and 5' CCCTGTTGCA**A**AGTTCACGCCG 3', in which the mutated nucleotides are indicated in bold, using the Dj6.4 cDNA as a template, to yield mutant core 1aY164F (fig 1B). PCR was carried out with the Pfu Turbo DNA polymerase (Stratagene, La Jolla CA). DNA sequencing was used to check that the original sequence was conserved in both constructs, and that the Y164F mutation had been correctly introduced.

Cell culture and RNA transfection

Baby hamster kidney cells (BHK-21) were cultured and electroporated with recombinant SFV RNA encoding the HCV core 1a or 1aY164F proteins, as previously described.[25-27] Briefly, cells were cultured at 37°C in Glasgow Minimal Essential Medium (GMEM) supplemented with 5% foetal calf serum and 2 % tryptose phosphate. For recombinant RNA synthesis, the various pSFV1 constructs were linearised by digestion at the *Spe*I restriction site, downstream from the 3' non-coding region of the SFV replicon. These constructs were then transcribed *in vitro* with SP6 RNA polymerase, making use of the SP6 promoter located upstream from the 5' extremity of the SFV replicon, as recommended by the manufacturer (Invitrogen). As a control, we synthesised a recombinant RNA encoding β-galactosidase (β-Gal). For transfection, 8 x 10^6 cells were mixed with 5 μg of recombinant SFV RNA and electroporated by a single pulse at 350 V, 750 mF (Easyject One, Eurogentec). Cells were cultured for 16 h following electroporation, as our previous studies have shown that the major morphological events associated with HCV structural protein production occur during this period in this system. [25 26] In some experiments, HCV core proteins were produced in BHK-21 cells in the presence of 100 μM of $(Z\text{-}LL)_2$-ketone (Calbiochem), an inhibitor of SPP.[27] All experiments were conducted with BHK-21 cells, except for confocal microscopy studies of the subcellular distribution of core proteins. For these studies, we transfected the human hepatocellular carcinoma cell line FLC4 under similar conditions. The lower efficiency of the SFV vectors in these cells resulted in the production of smaller amounts of protein than in BHK-21 cells, allowing a more precise analysis of the subcellular distribution of proteins.[27]

Western blotting

BHK-21 cells were lysed in a buffer containing protease inhibitors as previously described.[25-27] Samples were then separated by SDS-PAGE in 15 % polyacrylamide gels and the resulting bands were transferred to a polyvinylidene difluoride membrane. The membrane was blocked by incubation in 0.05 % (vol/vol) Tween 20 in PBS (PBS-T) supplemented with 5 % (wt/vol) skimmed milk powder. Membranes were incubated with the mouse monoclonal anti-HCV core C1856 antibody (Virostat, Portland, ME) diluted 1:5000 in PBS-T, washed and incubated with a horseradish peroxidase-conjugated anti-mouse antibody diluted 1:10000 in PBS-T. Antibody binding was detected by enhanced chemiluminescence (ECL Plus; Amersham Bioscience).

Core protein and lipid droplet staining for confocal microscopy

FLC4 cells grown on glass coverslips were washed with PBS and fixed by incubation for 30 minutes at room temperature in 4% paraformaldehyde in PBS. Cells were permeabilised by incubation for 30 min in 0.05% saponin, 0.2 % bovine serum albumin (BSA) in PBS. Cells were incubated with anti-HCV core C1856 antibody (1:50 in permeabilisation buffer), then washed in PBS and incubated with an anti-mouse secondary antibody coupled to Alexa Fluor 488 (Molecular Probes, Eugene, OR), diluted 1:1000 in permeabilisation buffer. For lipid staining, cells were treated with Nile red (Sigma Aldrich), diluted 1:1000 (from a 1 mg/ml stock solution in acetone) in permeabilisation buffer, during incubation with the secondary antibody. Cells were then washed and mounted for analysis under an Olympus Fluoview 500 confocal laser scanning microscope.

Electron microscopy and lipid droplet quantification

For standard electron microscopy (EM), transfected BHK-21 cells were fixed by incubation for 48 h in 4% paraformaldehyde and 1% glutaraldehyde in 0.1 M phosphate buffer (pH 7.2) and postfixed by incubation for 1 h with 2% osmium tetroxide (Electron Microscopy Science, Hatfield, PA). They were dehydrated in a graded series of ethanol solutions, cleared in propylene oxide, and embedded in Epon resin (Sigma), which was allowed to polymerise for 48 h at 60°C. Ultrathin sections were cut, stained with 5 % uranyl acetate 5 % lead citrate, and placed on EM grids coated with collodion. The sections were then observed with a Jeol 1010 transmission electron microscope (Tokyo, Japan) connected to a Gatan digital camera driven by Digital Micrograph software (Gatan, Pleasanton, CA) for image acquisition and analysis.

For immuno-EM, transfected BHK-21 cells were fixed by incubation in a solution containing 4% paraformaldehyde in 0.1 M phosphate buffer (pH 7.2) for 16 h. The cell pellet was then dehydrated in a graded series of ethanol solutions at –20°C, using an automatic freezing substitution system (AFS, Leica), and embedded in London resin white (Electron Microscopy Science). The resin was allowed to polymerise at –25°C, under UV light, for 72 h. Ultrathin sections were blocked by incubation with 1% fraction V bovine serum albumin (BSA, Sigma) in PBS. They were then incubated with anti-HCV core C1856 monoclonal antibody diluted 1:50 in PBS supplemented with 1% BSA, washed and incubated with 15 nm-gold particles conjugated to goat anti-mouse antibodies (British Biocell International, Cardiff, UK) diluted 1:40 in PBS supplemented with 0.1% BSA. We used conjugated goat secondary antibodies without prior incubation with primary antibody to check that the reaction was specific. Ultrathin sections were stained and observed as described above.

For each construct (β-Gal, core 1a, core 1aY164F), the number and diameter (in μm) of lipid droplets was determined on the computer screen for 100 consecutive EM (standard) sections of the transfected cells. All investigations were conducted blind, with the encoded EM grids examined in random order. Lipid droplet diameter was converted into an area in μm^2. By summing these areas, we were able to determine the cumulative lipid droplet area, in μm^2, for each cell section.

Statistical analysis

Lipid droplet areas in 100 consecutive EM sections of the transfected cells seemed to follow mixed distributions. Indeed, the probability of observing a null area (discrete component of the distribution) was non-null, whereas a probability density function existed for all non-zero values of cumulative areas (continuous component of the distribution). We therefore decided to categorise the variable before carrying out statistical tests. Based on Sturges' rule, we defined seven classes of cumulative lipid droplet area (0 μm^2; 0-0.5 μm^2; 0.5-1 μm^2; 1-2 μm^2; 2-3 μm^2; 3-5 μm^2 and >5 μm^2), thereby defining an ordinal variable. Constructs were compared, using a global chi-squared test, followed by chi-squared tests for trend, taking into account the ordinal nature of the newly created variables. Data were analysed with SAS 9.1 software.

RESULTS

Expression and processing of HCV core 1a and 1aY164F proteins

Sixteen hours after transfection with the constructs encoding HCV core proteins or the β-gal control, the cells were harvested and lysed for western-blot analysis (fig. 2A). Consistent with our previous findings,[26 27] the core 1a protein encoded by the Dj6.4 sequence was efficiently cleaved by SPP (fig. 2A line 2). As this cleavage leads to the removal of a short domain, it is difficult to discriminate between the cleaved and uncleaved forms of the HCV core protein on western blots.[31] We therefore used cells expressing the core 1a construct and treated with $(Z\text{-}LL)_2$-ketone, a commercially available inhibitor of SPP, as a control. As previously reported,[27] immunoblot analyses of cells treated with this inhibitor showed that SPP cleavage was only partially inhibited, leading to the detection of both p23 and p21. This made it possible to identify unambiguously the cleaved and uncleaved forms of the HCV core protein (fig. 2A line 3). The core 1a protein appeared to be fully cleaved in our system, as the protein was detected solely as a 21 kDa product. A similar result was obtained with the core 1aY164F protein (fig. 2A line 4). We used Image J software for gel analysis to quantify the wild-type and mutant core proteins in the scanned blot and found that these two proteins were present in similar amounts.

Colocalisation of HCV core proteins with lipid droplet.

Nile red labelling in cells transfected with the β-gal construct showed that lipids were evenly distributed throughout the cytoplasm (fig. 2B). Transfection with the core 1a construct induced the clustering of large lipid droplets in the perinuclear area. These droplets were strongly stained for HCV core protein, as previously reported for our model,[27] and for other *in vitro* cellular models.[20 29] The HCV core 1aY164F mutant induced a similar clustering of large lipid droplets and was distributed similarly to the core 1a protein (fig. 2B). Similar results were obtained when the experiment was repeated and for analyses of large numbers of cells (only one cell is shown for each construct in fig. 2B, to show the colocalisation of HCV core proteins and lipid droplets as clearly as possible). However, we cannot exclude the possibility that the HCV core 1a protein and the mutant 1aY164F protein induced subtle differences in lipid droplet clustering, undetectable by confocal microscopy. This technique was not considered appropriate for comparison and quantification of the lipid droplet accumulation induced by the two different HCV core constructs.

Electron microscopy and lipid droplet quantification

Standard electron microscopy showed that the ultrastructural changes observed in cells transfected with recombinant SFV vectors encoding the HCV core 1a and 1aY164F proteins

were consistent with the results of confocal microscopy with the clustering of large lipid droplets in the perinuclear area (fig. 3). No specific ultrastructural change was observed in cells producing a control protein (β-Gal, not shown). Immuno-electron microscopy showed that the surface of the clustered large lipid droplets stained strongly positive for HCV core protein, as previously described in other models[19] (fig. 3B). Preliminary experiments suggested that the lipid droplets induced by the HCV core 1aY164F protein tended to be larger and more numerous than those induced by the HCV core 1a protein (fig. 3). We determined the cumulative area of these lipid droplets for 100 consecutive cell sections, for each construct, studied in random order, with the observer blind to the construct used. As expected, the cumulative area of the lipid droplets was significantly greater for the wild-type HCV core protein than for β-gal ($p < 0.001$, fig. 4). This difference was accounted for mostly by the higher frequency of sections containing more than 2 μm^2 of lipid droplets for wild-type HCV core protein. None of the control cells had such a large lipid droplet area. The cumulative area of lipid droplets was significantly greater in cells producing the 1aY164F protein than in cells producing the wild-type HCV core 1a protein ($p < 0.001$, fig. 4). This difference resulted largely from the higher frequency of sections containing more than 3 μm^2 of lipid droplets for cells producing the HCV core 1aY164F protein. A significant proportion of these sections contained more than 5 μm^2 of lipid droplets, whereas only a tiny number of sections of cells producing the HCV core 1a protein displayed such large lipid droplet areas.

Discussion

In chronic hepatitis C, liver steatosis is significantly associated with genotype 3 viruses, although patients infected with viruses of other genotypes may also display virus-induced liver steatosis. Quantitative determination of HCV core protein levels in the liver of transgenic mice producing this protein has shown that steatosis grade is correlated with core protein levels, demonstrating that core protein plays a causal role in the pathogenesis of hepatic steatosis. Both *in vitro,* in transfected cells, and *in vivo,* in transgenic mice, HCV core protein has been shown, by confocal and/or electron microscopy, to be located at the surface of lipid droplets. However, all these investigations were conducted with viral sequences cloned from genotype 1 viruses.

We investigated the molecular basis of HCV genotype-related steatosis, using an *in vitro* cellular model to compare the effects of a wild-type 1a HCV core protein with those of a mutant (Y164F) protein with a genotype 3-specific residue (F at position 164). Lipid droplets

accumulated with both constructs, but cumulative lipid droplet area was significantly larger in cells transfected with the Y164F mutant than in cells transfected with the wild-type construct. This difference was not related to HCV core protein levels or SPP cleavage. Tyrosine and phenylalanine are both aromatic, hydrophobic residues. However, phenylalanine is more hydrophobic than tyrosine, from which it differs only in terms of the hydroxyl group present in the *ortho* position on the benzene ring of tyrosine. Unlike tyrosine, phenylalanine has a fairly non-reactive side chain, and is thus rarely involved in protein-protein interactions.[32] However, phenylalanine can play a role in substrate recognition, particularly for hydrophobic ligands, such as lipids.[32]

HCV core protein has been shown to decrease microsomal triglyceride transfer (MTP) protein activity in the HCV core transgenic mouse model, reducing the secretion of very low density lipoproteins (VLDL).[33] MTP is a luminal ER protein that acts as a major regulator of VLDL assembly. MTP stabilises apolipoprotein B (apoB) by lipidation, and the resulting lipidated apoB subsequently fuses with triglyceride-rich particles, leading to VLDL formation.[34] The impaired VLDL assembly and secretion induced by HCV core protein is thus associated with intracytoplasmic triglyceride storage in lipid droplets.[33] Although the HCV core of genotype 1a viruses has been shown to associate with several cellular proteins,[35] no direct binding to apoB, MTP or its cofactor PDI (protein disulphide isomerase, another luminal ER protein) has been demonstrated in yeast two-hybrid screening systems.[36] This suggests that HCV core protein-mediated MTP inhibition may involve interactions between HCV core protein and lipids, rather than proteins.[33 36] The HCV core may prevent lipids from interacting with MTP, thereby inhibiting the transfer of lipids to apoB. In addition, specific interactions between HCV core protein and the lipids of the ER membrane may hamper the MTP-mediated transfer of triglycerides to the ER lumen, leading to their accumulation in lipid droplets.[33 36] The F164 residue in the HCV core 1aY164F protein may therefore confer on this mutant protein a higher affinity for the lipids in the ER membrane. Recent structural studies of the HCV core protein (1a genotype) have shown that domain II is a membrane-binding domain containing two amphipathic α-helices extending from L119 to Y136 and A148 to Y164, which probably interact within the same plane at the interface of the two phospholipid layers of the ER membrane.[37-39] The tyrosine at position 164 in the HCV core protein is therefore thought to be located at the site of lipid droplet morphogenesis.[40] The replacement of this residue by a phenylalanine may increase the affinity of the HCV core protein for the

lipids present between the leaflets of the ER membrane, ultimately leading to higher level of lipid droplet formation.

In vitro cellular models have intrinsic limitations, but our results are consistent with a hypothesis formulated on the basis of clinical studies, according to which viral sequences have a direct effect on genotype 3-specific steatosis. [9 11-15] A similar conclusion was recently drawn in a study in which an HCV core protein sequence from a genotype 3 virus was expressed in a cellular model.[24] However, the authors were unable to identify the residue(s) involved in this phenomenon, and did not implicate F164. This difference in results may be due to the different cell models and lipid droplet quantification methods used in the two studies. We believe that the method used in our study, in which lipid droplet number and size were determined in consecutive EM sections, is the most accurate way to quantify lipid accumulation in cells. However, we cannot exclude the possibility that other residues differing between the HCV core sequences used in these studies may modulate the role of the F164 in intracellular lipid accumulation. We intend to test this hypothesis in futures studies, by investigating aa changes both in the domain II and in the other HCV core protein domains. It will also be interesting to express HCV core sequences cloned from patients infected with various genotype 3 viruses and compare their abilities to induce lipid droplet accumulation *in vitro*.

In conclusion, our study provides a molecular explanation for genotype 3-specific HCV-related lipid accumulation in the liver. Genotype 3 may behave differently from other genotypes due to its phenylalanine residue, which has a higher affinity for lipids than tyrosine. It has been shown that single aa changes due to mutations in HCV core genes cloned from hepatocellular carcinoma samples can radically alter the biological activity of the protein.[41] Our study provides an additional example of the pathogenic potential of HCV core genetic variability, and may help to guide future studies of the mechanisms involved in the pathogenesis of HCV-induced liver steatosis.

ACKNOWLEDGEMENTS

We thank Yoshiharu Matsuura (Research Institute for Microbial Diseases, Osaka, Japan) for providing us with the FLC4 cell line. This work was supported by grants from the Ligue Contre le Cancer (Comité d'Indre & Loire et Comité du Cher) and ANRS (Agence Nationale de Recherche sur le SIDA et les hepatites virales). Our research is supported by the Region Centre (Equipe ESPRI). R.P. was supported by a fellowship from the French Ministry of

Research. Our data were obtained with the assistance of the RIO Electron Microscopy Facility of François Rabelais University.

Competing interests: None to declare

REFERENCES

1 **Alter MJ**, Mast EE, Moyer LA, *et al.* Hepatitis C. *Infect Dis Clin North Am* 1998; **12**:13-26.

2 **Simmonds P.** Genetic diversity and evolution of hepatitis C virus-15 years on. *J Gen Virol* 2004; **85:**3173-88.

3 **Rehermann B.** Interaction between the hepatitis C virus and the immune system. *Semin Liver Dis* 2000; **20**: 127-41.

4 **Goodman ZD**, Ishak KG. Histopathology of hepatitis C virus infection. *Semin Liver Dis* 1995 ; **15**:70-81.

5 **Powell EE**, Jonsson JR, Clouston AD. Steatosis: co-factor in other liver diseases. *Hepatology* 2005; **42**:5-13.

6 **Fartoux L**, Chazouilleres O, Wendum D, *et al*. Impact of steatosis on progression of fibrosis in patients with mild hepatitis C. *Hepatology* 2005; **41**:82-7.

7 **Castera L**, Hezode C, Roudot-Thoraval F, *et al*. Worsening of steatosis is an independent factor of fibrosis progression in untreated patients with chronic hepatitis C and paired liver biopsies. *Gut* 2003; **52**:288-92.

8 **Hourigan LF**, Macdonald GA, Purdie D, *et al.* Fibrosis in chronic hepatitis C correlates significantly with body mass index and steatosis. *Hepatology* 1999; **29**:1215-9.

9 **Monto A**, Alonzo J, Watson JJ, *et al*. Steatosis in chronic hepatitis C: relative contributions of obesity, diabetes mellitus, and alcohol. *Hepatology* 2002; **36:**729-36.

10 **Fartoux L**, Poujol-Robert A, Guechot J, *et al*. Insulin resistance is a cause of steatosis and fibrosis progression in chronic hepatitis C. *Gut* 2005; **54:**1003-8.

11 **Rubbia-Brandt L,** Quadri R, Abid K, *et al*. Hepatocyte steatosis is a cytopathic effect of hepatitis C virus genotype 3. *J Hepatol* 2000; **33**:106-15.

12 **Rubbia-Brandt L**, Fabris P, Paganin S, *et al*. Steatosis affects chronic hepatitis C progression in a genotype specific way. *Gut* 2004, **53**:406-12.

13 **Adinolfi LE**, Gambardella M, Andreana A, *et al*. Steatosis accelerates the progression of liver damage of chronic hepatitis C patients and correlates with specific HCV genotype and visceral obesity. *Hepatology* 2001; **33**:1358-64.

14 **Castera L**, Hezode C, Roudot-Thoraval F, *et al*. Effect of antiviral treatment on evolution of liver steatosis in patients with chronic hepatitis C: indirect evidence of a role of hepatitis C virus genotype 3 in steatosis. *Gut* 2004; **53**:420-4.

15 **Kumar D**, Farrell GC, Fung C, George J. Hepatitis C virus genotype 3 is cytopathic to hepatocytes: Reversal of hepatic steatosis after sustained therapeutic response. *Hepatology* 2002; **36**:1266-72.

16 **Asselah T**, Rubbia-Brandt L, Marcellin P, Negro F. Steatosis in chronic hepatitis C: why does it really matter? *Gut* 2006; **55**:123-30.

17 **Poynard T**, Ratziu V, McHutchison J, *et al*. Effect of treatment with peginterferon or interferon alfa-2b and ribavirin on steatosis in patients infected with hepatitis C. *Hepatology* 2003; **38**:75-85.

18 **Moradpour D**, Englert C, Wakita T, Wands JR. Characterization of cell lines allowing tightly regulated expression of hepatitis C virus core protein. *Virology* 1996; **222**:51-63.

19 **Barba G**, Harper F, Harada T, *et al*. Hepatitis C virus core protein shows a cytoplasmic localization and associates to cellular lipid storage droplets. *Proc Natl Acad Sci USA 1997*; **94**:1200-5.

20 **Hope RG**, McLauchlan J. Sequence motifs required for lipid droplet association and protein stability are unique to the hepatitis C virus core protein. *J Gen Virol* 2000; **81**:1913-25.

21 **Shi ST**, Polyak SJ, Tu H, *et al*. Hepatitis C virus NS5a colocalizes with the core protein on lipid droplets and interacts with apolipoproteins. *Virology* 2002; **292:** 198-210.

22 **Moriya K**, Yotsuyanagi H, Shintani Y, *et al*. Hepatitis C virus core protein induces hepatic steatosis in transgenic mice. *J Gen Virol* 1997; **78**:1527-31.

23 **Moriya K**, Fujie H, Shintani Y, *et al*. The core protein of hepatitis C virus induces hepatocellular carcinoma in transgenic mice. *Nat Med* 1998; **4**:1065-7.

24 **Abid K**, Pazienza V, de Gottardi A, *et al*. An in vitro model of hepatitis C virus genotype 3a-associated triglycerides accumulation. *J Hepatol* 2005; **42:**744-51.

25 **Blanchard E**, Brand D, Trassard S, *et al*. Hepatitis C virus-like particle morphogenesis. *J Virol* 2002; **76:** 4073-9.

26 **Blanchard E**, Hourioux C, Brand D, *et al*. Hepatitis C virus-like particle budding: role of the core protein and importance of its Asp111. *J Virol* 2003; **77**:10131-8.

27 **Ait-Goughoulte M**, Hourioux C, Patient R, *et al*. Core protein cleavage by signal peptide peptidase is required for hepatitis C virus-like particle assembly. *J Gen Virol* 2006; **87**:855-60.

28 **Liu Q**, Tackney C, Bhat RA, *et al*. Regulated processing of hepatitis C virus core protein is linked to subcellular localization. *J Virol* 1997; **71**:657-62.

29 **McLauchlan J**, Lemberg MK, Hope G, Martoglio B. Intramembrane proteolysis promotes trafficking of hepatitis C virus core protein to lipid droplets. *EMBO J* 2002; **21**:3980-8.

30 **Kuiken C**, Yusim K, Boykin L, Richardson R. The Los Alamos HCV sequence database. *Bioinformatics* 2005; **21**: 379-84.

31 **Hope RG**, McElwee MJ, McLauchlan J. Efficient cleavage by signal peptide peptidase requires residues within the signal peptide between the core and E1 proteins of hepatitis C virus strain J1. *J Gen Virol* 2006; **87**: 623-627.

32 **Betts MJ**, Russell RB. Amino acid properties and consequences of substitutions. In: Barnes MR, Gray IC, eds. *Bioinformatics for Geneticists*. Wiley, 2003.

33 **Perlemuter G**, Sabile A, Letterton P, *et al*. Hepatitis C virus core protein inhibits microsomal triglyceride transfer protein activity and very low density lipoprotein secretion: a model of viral-related steatosis. *FASEB J* 2002; **16:** 185-94.

34 **Raabe M**, Veniant MM, Sullivan MA, *et al*. Analysis of the role of microsomal triglyceride transfer protein in the liver of tissue-specific knockout mice. *J Clin Invest* 1999; **103:** 1287-98.

35 **McLauchlan J.** Properties of the hepatitis C virus core protein: a structural protein that modulates cellular processes. *J Viral Hepat* 2000; **7**: 2-14.

36 **Sabile A**, Perlemuter G, Bono F, *et al*. Hepatitis C virus core protein binds to apolipoprotein AII and its secretion is modulated by fibrates. *Hepatology* 1999; **30:** 1064-76.

37 **Boulant S**, Vanbelle C, Ebel C, *et al*. Hepatitis C virus core protein is a dimeric alpha-helical protein exhibiting membrane protein features. *J Virol* 2005; **79**: 11353-65.

38 **Suzuki R**, Sakamoto S, Tsutsumi T, *et al*. Molecular determinants for subcellular localization of hepatitis C virus core protein. *J Virol* 2005; **79**: 1271-81.

39 **Boulant S**, Montserret R, Hope G, *et al*. Structural determinants that target the hepatitis C virus core protein to lipid droplets. *J Biol Chem* 2006; **281**: 22236-47.

40 **Martin S**, Parton R. Lipid droplets: a unified view of a dynamic organelle. *Nat Rev Mol Cell Biol* 2006; **7**: 373-8.

41 **Delhem N**, Sabile A, Gajardo R, et al. Activation of the interferon-inducible protein kinase PKR by hepatocellular carcinoma derived-hepatitis C virus core protein. *Oncogene* 2006; **20**: 5836-45.

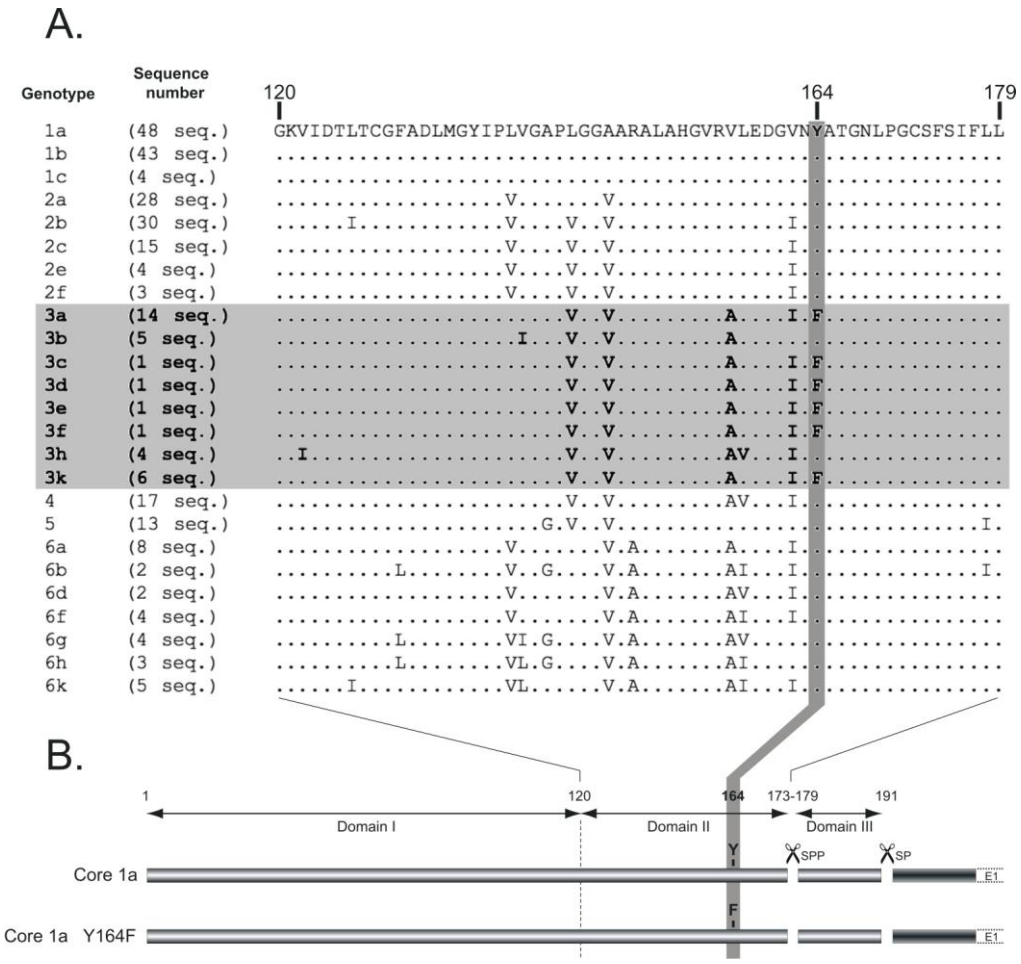

Figure 1 Alignment of domain II of HCV core proteins from different genotypes and design of the constructs. (A) 266 different sequences from the 6 HCV genotypes, including 25 subtypes, were aligned, using the Los Alamos National Laboratory HCV database web interface. Depending on the subtype, the number of available sequences varied from 1 to 48 (number in brackets). When more than one sequence was available for a given subtype, the database interface provided a consensus sequence for this subtype. The phenylalanine (F) at position 164 was the only residue specific to HCV genotype 3. (B) The SFV wild-type HCV core construct for genotype 1a (core 1a) encoded the 191 aa of the core protein (C191) and the 27 N-terminal aa of the E1 envelope protein; a similar SFV construct encoding a mutant Y164F (core 1aY164F) was obtained from the wild-type sequence, by site-directed mutagenesis. SPP: signal peptide peptidase; SP: signal peptidase.

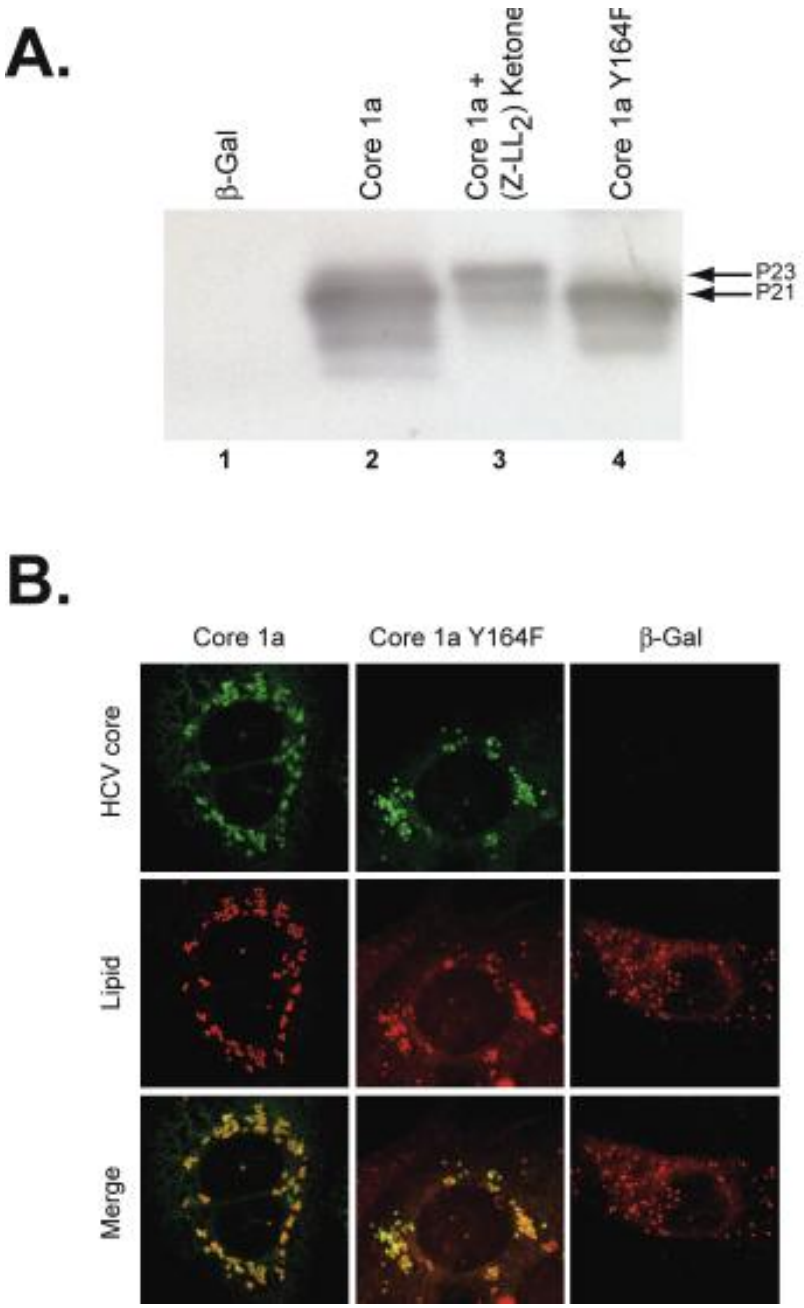

Figure 2 Analysis of HCV core 1a and 1aY164F protein production and subcellular distribution. (A) Production, in BHK-21 cells, of the β-galactosidase, HCV core 1a and 1aY164F proteins, and western-blot analysis of their processing, using a monoclonal anti-HCV core antibody. Wild-type core 1a protein production was assessed in the presence and absence of the SPP inhibitor $(Z\text{-}LL)_2$ ketone, to make it possible to visualise the uncleaved (p23) and cleaved (p21) forms of the core protein. (B) Confocal microscopy analysis of the fluorescence of the HCV core 1a and 1aY164F proteins, using a monoclonal anti-HCV core antibody, combined with the Nile red staining of lipid droplets in FLC4 cells.

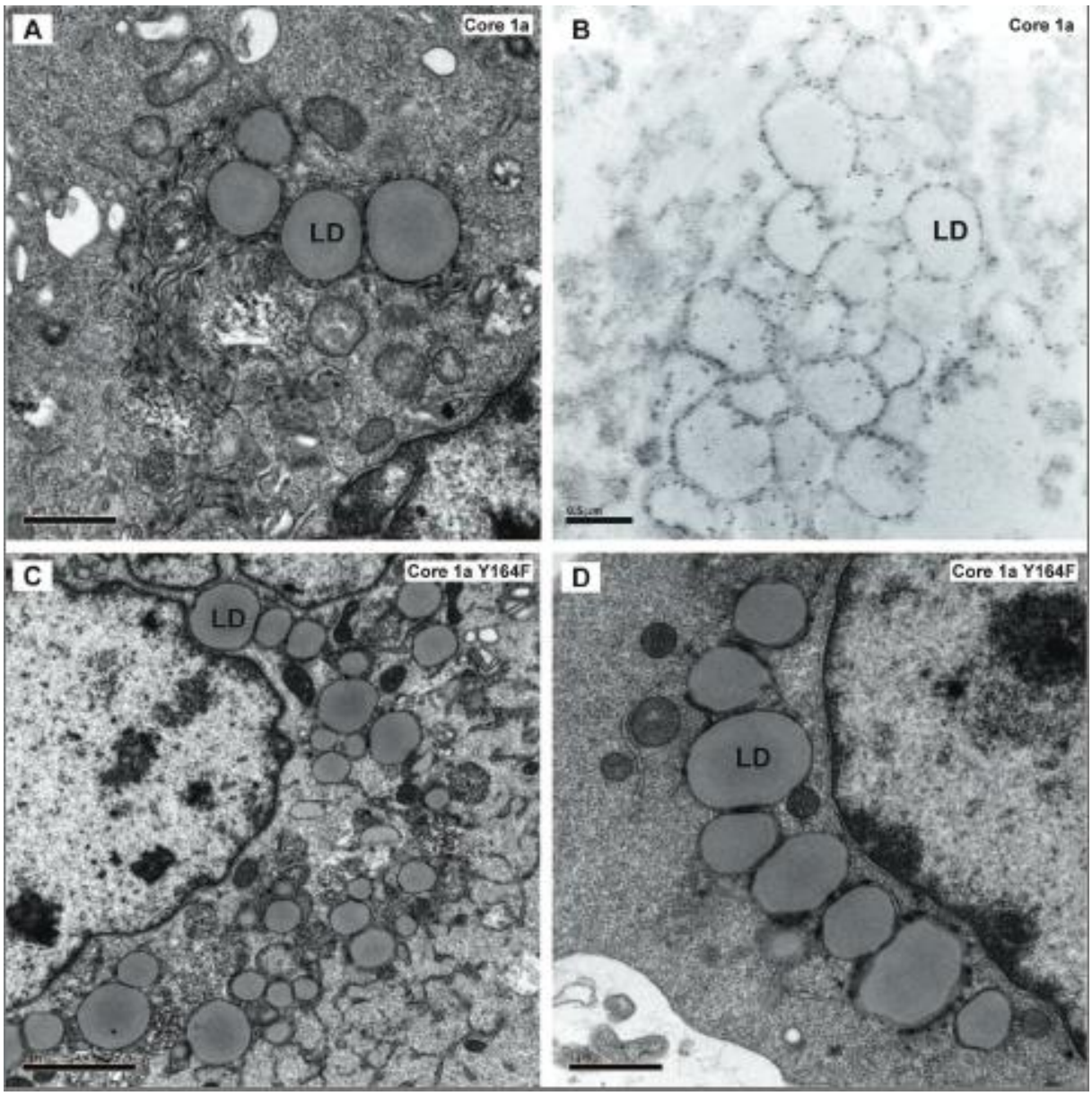

Figure 3 Electron micrographs of BHK-21 cells producing the HCV core 1a and 1aY164F proteins. The micrographs show typical clusters of lipid droplets (LD) in the perinuclear area of cells producing the core 1a protein (A) and the core 1aY164F protein (C and D). (B) Freeze substitution EM immunogold labelling with a monoclonal anti-HCV core antibody demonstrated the presence of large amounts of core protein (core 1a in this section) at the surface of the clustered lipid droplets. Bars = 1 μm in A and D, 0.5 μm in B, 2 μm in C.

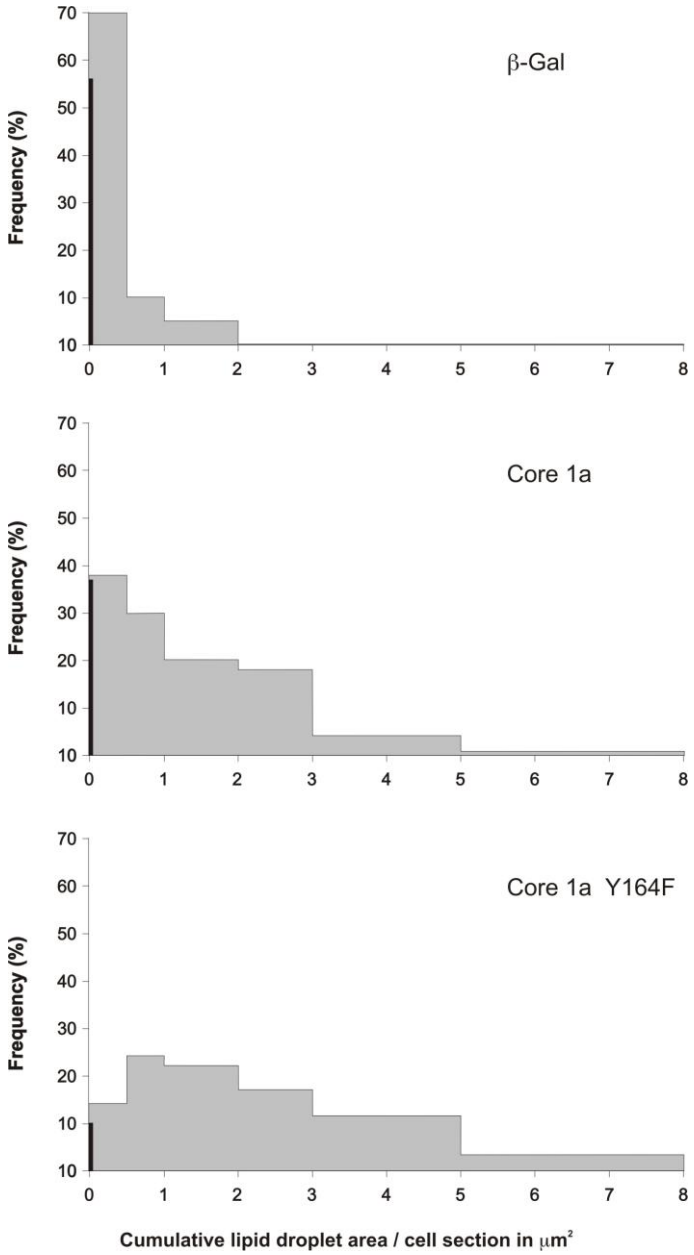

Figure 4 Quantification of the cumulative area of lipid droplets in sections of cells producing the β-galactosidase, HCV core 1a and 1aY164F proteins. The cumulative area of lipid droplets per cell section (in μm^2) was determined blindly for coded EM grids examined in random order and corresponding to 100 consecutive cell sections for each protein. Cumulative lipid droplet area was categorised into seven classes: 0 μm^2; 0-0.5 μm^2; 0.5-1 μm^2; 1-2 μm^2; 2-3 μm^2; 3-5 μm^2 and >5 μm^2. The probability distributions were mixed distributions. The thick line in 0 indicates the frequency of null areas, whereas non-null areas are presented as histograms. The chi-squared test associated with the global comparison of the three constructs yielded a p value lower than 0.001. All pair-wise comparisons (chi-squared tests of trend) yielded to p values lower than 0.001.